



Efficiency Correction Is Required for Accurate Quantitative PCR Analysis and Reporting

Jan M. Ruijter,^{a,*} Rebecca J. Barnewall,^{b,c} Ian B. Marsh,^d Andrew N. Szentirmay,^e Jane C. Quinn,^{b,c}
Robin van Houdt,^f Quinn D. Gunst,^a and Maurice J.B. van den Hoff^{a,*}

BACKGROUND: Quantitative PCR (qPCR) aims to measure the DNA or RNA concentration in diagnostic and biological samples based on the quantification cycle (C_q) value observed in the amplification curves. Results of qPCR experiments are regularly calculated as if all assays are 100% efficient or reported as just C_q , ΔC_q , or $\Delta\Delta C_q$ values.

CONTENTS: When the reaction shows specific amplification, it should be deemed to be positive, regardless of the observed C_q . Because the C_q is highly dependent on amplification efficiency that can vary among targets and samples, accurate calculation of the target quantity and relative gene expression requires that the actual amplification efficiency be taken into account in the analysis and reports. PCR efficiency is frequently derived from standard curves, but this approach is affected by dilution errors and hampered by properties of the standard and the diluent. These factors affect accurate quantification of clinical and biological samples used in diagnostic applications and collected in challenging conditions. PCR efficiencies determined from individual amplification curves avoid these confounders. To obtain unbiased efficiency-corrected results, we recommend absolute quantification with a single undiluted calibrator with a known target concentration and efficiency values derived from the amplification curves of the calibrator and the unknown samples.

SUMMARY: For meaningful diagnostics or biological interpretation, the reported results of qPCR experiments should be efficiency corrected. To avoid ambiguity, the Minimal Information for Publications on Quantitative

Real-Time PCR Experiments (MIQE) guidelines checklist should be extended to require the methods that were used (1) to determine the PCR efficiency and (2) to calculate the reported target quantity and relative gene expression value.

Introduction

Amplification of DNA in PCR can be monitored in real time with fluorescent DNA-binding dyes or sequence-specific probes (1, 2). The term “real-time PCR” was originally introduced and is still used in PCR-based microbial diagnostics (3). To avoid confusion about the abbreviation RT, it is recommended to use the terms *qPCR* for quantitative real-time PCR measuring DNA and *RT-qPCR* for measuring RNA levels after reverse transcription (4). In this review, qPCR is used to describe PCR experiments or diagnostic assays regardless of the input nucleic acid.

Although several studies provide information on how to design (5), standardize (6, 7), and report qPCR experiments (4), they fail to adequately address the impact of differences in PCR efficiency among assays, standards, and samples. Most qPCR reports provide only quantification cycle (C_q) values as the result of a qPCR measurement and ignore the PCR efficiency or assume 100% efficiency for all reactions. The validity of this assumption for quantitative, as well as qualitative, outcomes of published experiments often cannot be checked by reviewers and readers (4). This approach becomes even more relevant when targets are evaluated in clinical or environmental samples with limited or no sample purification, and thus with individual characteristics and compositions that may affect PCR efficiency.

The current review describes how the validity of reported qPCR results is affected by ignoring that PCR efficiencies are <100% and may be different among assays, samples, and standards. It also describes why a standard curve and an amplification curve analysis often result in different PCR efficiencies for the same assay. Equations were derived to enable calculation of biasing effects of differences in PCR efficiency on reported results and the effects of dilution errors on the standard

^aDepartment of Medical Biology, Amsterdam University Medical Centres, Location Academic Medical Center, Amsterdam, the Netherlands; ^bSchool of Animal and Veterinary Sciences, Charles Sturt University, Wagga Wagga, NSW, Australia; ^cNSW Department of Primary Industries, Graham Centre for Agricultural Innovation, Charles Sturt University, Wagga Wagga, NSW, Australia; ^dNew South Wales Department of Primary Industries, Elizabeth Macarthur Agricultural Institute, Narellan, NSW, Australia; ^eGene Target Solutions, Dural, NSW, Australia; ^fDepartment of Medical Microbiology and Infection Prevention, Amsterdam University Medical Centres, Amsterdam, the Netherlands.

*Address correspondence to this author at: Department of Medical Biology, Amsterdam University Medical Centres, Location Academic Medical Center, Meibergdreef 15, 1105AZ Amsterdam, the Netherlands. E-mail m.j.vandenhoff@amsterdamumc.nl.

Received December 15, 2020; accepted March 19, 2021.

DOI: 10.1093/clinchem/hvab052

curve-derived PCR efficiency. Because PCR efficiency values for individual reactions and samples are never published, this review includes a reanalysis of existing data sets to illustrate this variation in PCR efficiencies. The online [Supplemental Excel File](#) enables the reader to evaluate the effects of different parameter values on reported results or personal data.

qPCR Analysis Principle

All symbols used in this review conform to the recommendations of the Minimal Information for Publications on Quantitative Real-Time PCR Experiments (MIQE) guidelines (4). Amplification efficiency is defined as fold increase per cycle with a value between 1 and 2, with 2-fold being a 100% efficient PCR. The basic equation for PCR kinetics (Eq. 1) states that the number of target copies after c cycles (N_c) is the starting number of targets (N_0) times the PCR efficiency (shown as E) to the power c :

$$N_c = N_0 E^c. \quad \text{Eq. 1}$$

To assess the exponential phase, the fluorescence axis of the amplification curve graph needs to be plotted on a logarithmic scale. The logarithmic form of Eq. 1, ($\log(N_c) = \log(N_0) + \log(E) \times c$), shows that the amplification curve is a straight line until the end of the exponential phase (Fig. 1, A), with a slope determined by a constant PCR efficiency (8). During the exponential phase, the observed fluorescence is proportional to the DNA concentration (9, 10). Extrapolation of the exponential phase down to cycle 0 reflects the early cycles of amplification. Its intercept with the fluorescence axis represents the fluorescence associated with N_0 (Fig. 1, A). This visualization of early amplification curves will be used to illustrate the effects of different PCR efficiency values.

The number of cycles required to reach the preset fluorescence quantification threshold (N_q) is defined as the C_q (4). Therefore, C_q is an indirect measure for the target quantity in the reaction. After determining C_q , the researcher can either draw a qualitative conclusion or continue with a quantitative analysis.

Qualitative Interpretation of C_q in Diagnostics

To illustrate the wide range of efficiency and C_q values observed in a routine clinical diagnostic test, we retrieved data from 1 week of validated probe-based COVID-19 PCR tests (online [Supplemental Dataset 1](#)). All negative controls and 1037 patient samples were negative, ruling out contamination of reaction components (11). In this clinical application, 85 samples were considered positive because the observed fluorescence increased above the quantification threshold. This approach is hampered by the fact that qPCR machines set

different quantification thresholds that can differ between runs and can be manually overruled by the user when required (online [Supplemental Excel File](#), Sheet 1) (6). After reanalysis with a constant threshold, the 85 positive samples showed a wide range of C_q values (Fig. 2, A). It is a general contention that these differences in C_q values reflect differences in the number of copies of the virus in the reactions. Although C_q is related to the target concentration, this relation depends heavily on the PCR efficiency; amplification with a low efficiency takes more cycles to reach the quantification threshold (Fig. 1, A). Because high C_q values may result from low-efficiency PCRs, arbitrary C_q cutoffs, even above 40 cycles, are not recommended (4).

When a sample is pipetted into a reaction well, an unavoidable sampling variation, governed by the Poisson distribution, occurs. Especially with low target concentration, technical replicates will always result in a range of actual input values and thus C_q values. For reactions with an input below 10 copies of target, the number of reactions with an unexpected high C_q and those without amplification will increase (online [Supplemental Background 1](#); [Supplemental Excel File](#), Sheet 2). With a validated probe-based assay, the presence of amplification means that the target was present and the sample can be diagnosed as positive. When a DNA-binding dye is used, samples above a C_q of 27 are suspect because of the frequent occurrence of amplification artifacts (15). However, because of the unavoidable Poisson variation, the absence of amplification is never a valid criterion to label a reaction as negative.

Quantitative Use of C_q in Gene Expression Analysis

After C_q cycles, when the PCR reaches N_q , Eq. 1 can be written as:

$$N_q = N_0 E^{C_q}. \quad \text{Eq. 2 (8)}$$

The efficiency-corrected N_0 per reaction can then be calculated by rearranging Eq. 2 into:

$$N_0 = N_q / E^{C_q}. \quad \text{Eq. 3 (16)}$$

When there are technical replicates, the average N_0 per biological sample is calculated and used for further analysis (17). A comparison of amplification curve analysis methods, using efficiency values either per assay or per reaction, showed that the least variable and most accurate results were obtained when the PCR efficiency of the assay was used in Eq. 3 (18).

In a logarithmic plot of the amplification curve, Eq. 3 mathematically describes the extrapolation of the exponential phase down to cycle 0; the intercept with the y axis is the logarithm of the fluorescence associated

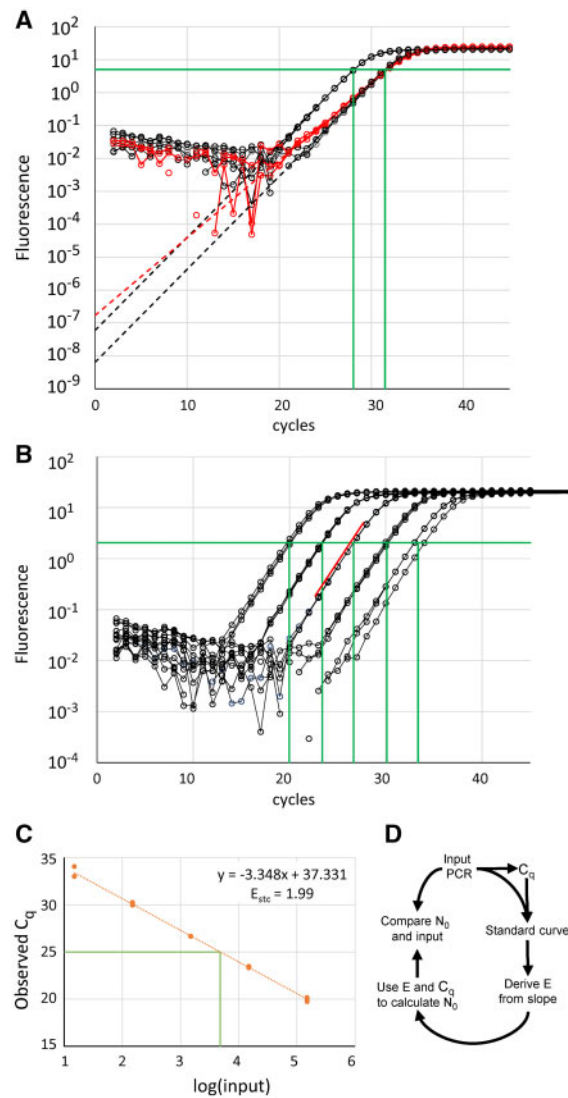


Fig. 1. (A), Relation between C_q and PCR efficiency. After baseline correction and plotting on a logarithmic fluorescence axis, the exponential phase of the amplification curve is represented by data points on a straight line; its slope is determined by the PCR efficiency. Extrapolation of this straight line to cycle 0 (dotted lines) intersects the y axis at the fluorescence associated with the target quantity (N₀). After setting N_q (green horizontal line), the C_q values can be determined (vertical green lines). The graph shows 2 reactions (black) that are amplified with the same efficiency; consequently, their ΔC_q is directly related to the fold difference in target quantities. The third reaction (red) is amplified with a lower PCR efficiency; it has the same C_q value as the low concentration of the black reaction, but its target quantity is >10-fold higher. (B), Amplification curves of a dilution series. The amplification data shown are from triplicate measurements of a 10-fold dilution series with 150 000 down to 15 copies per reaction. The vertical lines indicate the C_q values per dilution. The red line highlights the slope of the exponential phase which is used to determine the PCR efficiency from individual amplification curves (Eq. 9). (C), Standard curve. The C_q values observed in (B) are plotted against the logarithm of the input concentration of each reaction. The PCR efficiency is then derived from the slope of the regression line fitted to the data points (Eq. 8). The green horizontal and vertical lines in (C) illustrate the use of the dilution series as a calibration curve (online [Supplemental Background 5](#)). An observed C_q value of 25, for example, translates into a log(N₀) of 3.683, which is a target quantity of 4823 copies. Despite this seemingly exact result, the researcher should consider the uncertainty of the calibration curve in the reported results. (D), Schematic illustration of the circular reasoning in the standard curve approach. The correlation between the output and the input does not show the unbiasedness of this approach but shows only that what goes in does come out.

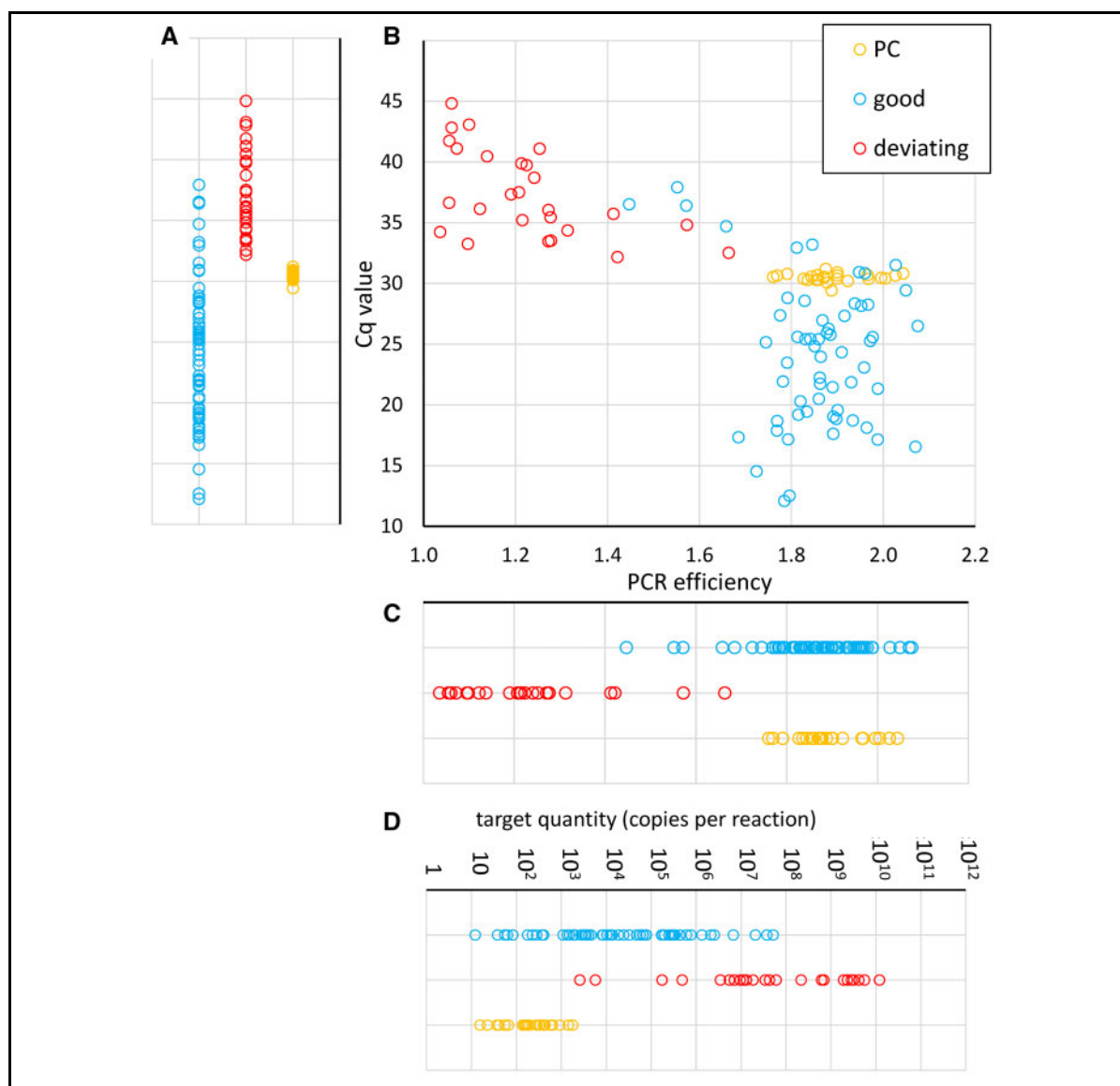


Fig. 2. Analysis of COVID-19 qPCR data. In total, 1122 COVID-19 qPCR tests were performed in 24 runs, each with one positive control (PC, orange marker) and one negative control (NC). Of those PCRs, 85 were deemed positive because they reached N_q , and a C_q value was determined. However, 26 of those reactions did not reach the plateau phase or did not show a monotonically increasing exponential phase (online [Supplemental Dataset 1](#)). In these 26 low-quality reactions (red marker), the PCR efficiency was derived as the fold increase around the observed C_q value (12). The other 59 positive reactions (blue marker) showed good amplification curves, and their PCR efficiency could be determined from the slope of the exponential phase. Note that the axis of (A) is the y axis of (B), and the axis of (C) is the x axis of (B). (A), Distribution of observed C_q values. (B), Scatterplot of the C_q value and PCR efficiency of the 85 positive reactions. Note that there is no systematic relation between C_q value and PCR efficiency within each of the 3 groups of reactions. (C), Distribution of PCR efficiency values. (D), Distribution of target number per reaction calculated for all positive reactions (N_0 , Eq. 3). The fluorescence at threshold was converted into the number of target copies with the rule of thumb that 10 copies in the reaction will result in C_q of 35 cycles (13, 14). Note that the deviating amplification curves have such low PCR efficiency that the calculated target quantity is too high to make sense, which shows that these reactions cannot be used to infer quantitative information.

with the starting concentration of the target in the reaction (Fig. 1, A). Converting these fluorescence values into number of target copies is not required in relative quantification because in the calculations, the fluorescence units cancel out (8).

Unwanted differences in sample size and composition have to be corrected by normalization (4, 19, 20). This requires measurement of N_0 of at least one but preferably several validated reference genes (21, 22). Normalized expression (i.e., $N_{0, tar}/N_{0, ref}$) is then calculated per biological sample. When multiple reference genes are measured, a proportional contribution of each is achieved by calculating the geometric mean of their target quantities (17, 21).

To calculate the fold change induced by a biological condition or experimental treatment, the normalized expression in the treated samples is divided by that in the control samples (Eq. 4):

$$\text{Fold effect} = \left(\frac{N_{0, tar, tr}}{N_{0, ref, tr}} \right) / \left(\frac{N_{0, tar, co}}{N_{0, ref, co}} \right). \quad \text{Eq. 4}$$

The handling of Eq. 4 with multiple reference genes is described in online Supplemental Background 2. Because the issues discussed in this review do not depend on the number of references, we show equations with only one reference gene.

Substitution of Eq. 3 into Eq. 4 cancels out N_q and, after rearrangement, results in the by now classic equation for efficiency-corrected relative quantification:

$$\text{Fold effect} = \frac{E_{tar}^{\Delta C_{q, tar}(co-tr)}}{E_{ref}^{\Delta C_{q, ref}(co-tr)}}. \quad \text{Eq. 5 (23)}$$

In Eq. 5, ΔC_q indicates the difference between the mean C_q in control and treatment groups for the target as well as the reference. To handle C_q values of more than one reference gene, the calculation becomes more complicated (10, 24–26).

In qPCR reports, the efficiency of an assay is often assumed to be 100%. In that case, Eq. 5 simplifies to $\text{Fold effect} = 2^{-(\Delta C_{q, tar}(co-tr) - \Delta C_{q, ref}(co-tr))}$. This equation is known as the $\Delta\Delta C_q$ equation and is mostly written as

$$\text{Fold effect} = 2^{-\Delta\Delta C_q}. \quad \text{Eq. 6 (27)}$$

The $\Delta\Delta$ symbols represent the difference in the difference in C_q values between target and reference genes under the control and experimental conditions (27).

The basic principle of qPCR is that ΔC_q , the difference in number of cycles with which 2 reactions reach the quantification threshold, directly reflects the fold difference in starting concentrations (8). However, this principle is true only when the PCR efficiencies of both reactions are equal (Fig. 1, A). Although this is frequently true for the same assay, different assays have different PCR efficiencies. The original report proposing

the $2^{-\Delta\Delta C_q}$ simplification describes a test to determine whether PCR efficiencies are sufficiently similar (27). However, an increasing number of studies report C_q , ΔC_q , or $\Delta\Delta C_q$ values and sometimes different, unused PCR efficiencies. This trend prompted the proposal to remove the dependency of C_q on PCR efficiency by publishing efficiency-adjusted C_q values (28). However, this proposal did not reach the mainstream of qPCR. Consequently, the reader can interpret the reported C_q data only by assuming that the PCR efficiency for all targets was 100%. This assumption has introduced biases and might underlie reported problems with the reproducibility of qPCR results.

Biased Interpretation of Reported ΔC_q Results

The following example illustrates the bias introduced by omitting the PCR efficiency from the qPCR analysis (Fig. 3; online Supplemental Background 3; Supplemental Excel File, Sheet 3). Figure 3, A illustrates the above-mentioned interpretation of the reported ΔC_q . Because all 3 treatments show a ΔC_q of -3 between genes A and B, each gene expression ratio will be interpreted to be 8 ($= 2^{-\Delta C_q}$), and the reader will conclude that there is no difference among treatments. The large differences in absolute expression levels among treatments have vanished.

Although the original report does not provide a definitive criterion for the point at which efficiencies are sufficiently similar to apply the $2^{-\Delta C_q}$ equation, the example given in that report suggests that a 2% efficiency difference is acceptable (27). When this small difference is present, the reported ΔC_q values result from gene expression ratios between 5.9 and 10.4 (Fig. 3, B). The “reported” ratio of 8 is then a 35% overestimation or 24% underestimation.

The seminal study on the design of qPCR experiments (6) gives a range of acceptable standard curve slopes that translate into efficiency values between 1.93 and 2.05. With these efficiencies, the gene expression ratios that give the reported ΔC_q actually range from 1.45 to 42.6 (Fig. 3, C), and the interpreted gene expression ratio is >5 times over- or underestimated. In our experience, PCR efficiencies in validated assays range from 1.70 to 1.91 (e.g., Fig. 4). With these efficiency values, the actual gene expression ratios range from 0.25 to 139 (Fig. 3, D). To explore other efficiency and C_q values, equations were derived to calculate and illustrate the bias in target quantity, expression ratio, and fold difference resulting from assuming an efficiency of 2 rather than using the actual efficiency in the data analysis (online Supplemental Background 3; Supplemental Excel File, Sheets 4–6)

Taken together, reporting just C_q values and requiring readers to assume a PCR efficiency of 2 to

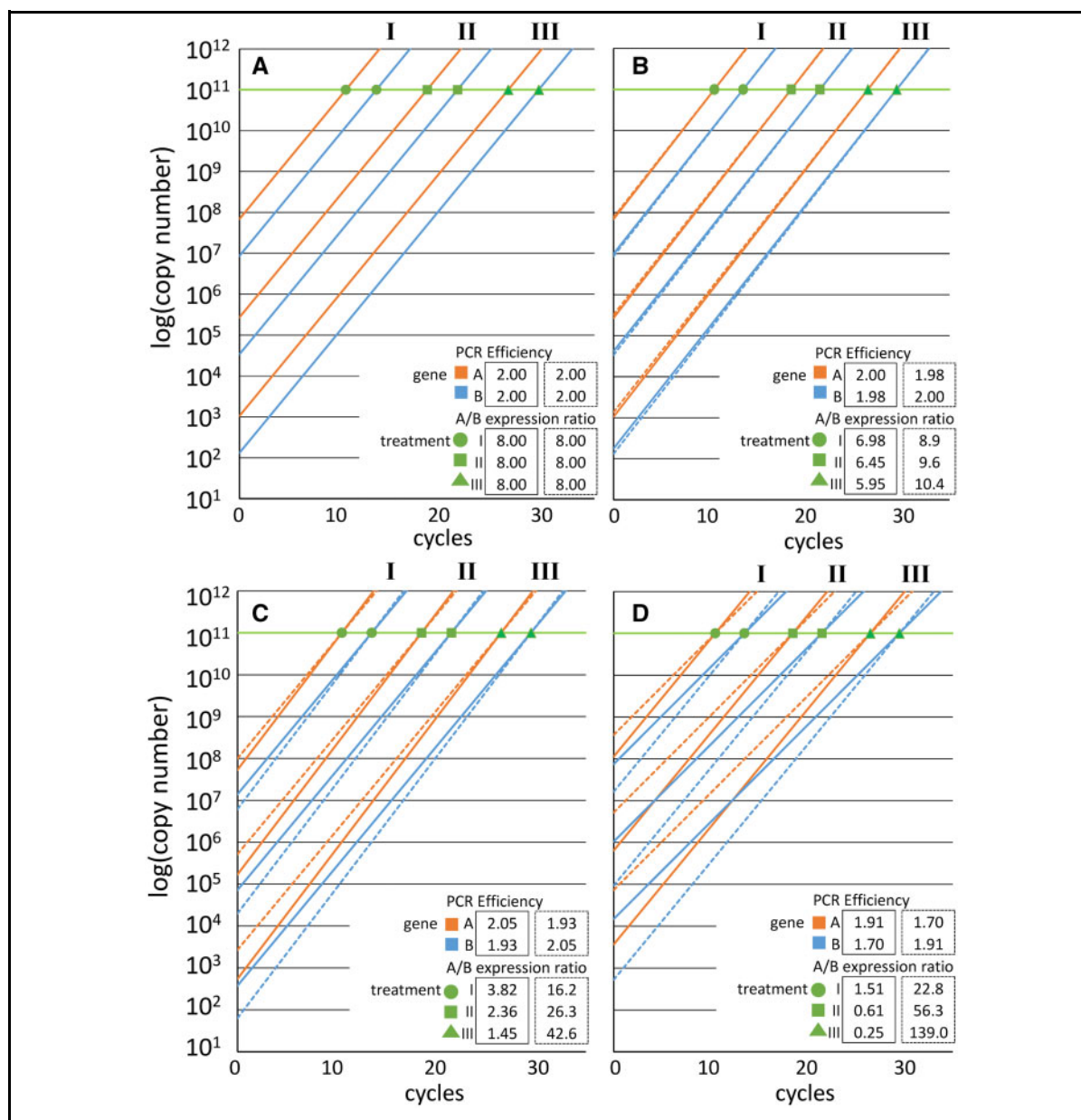
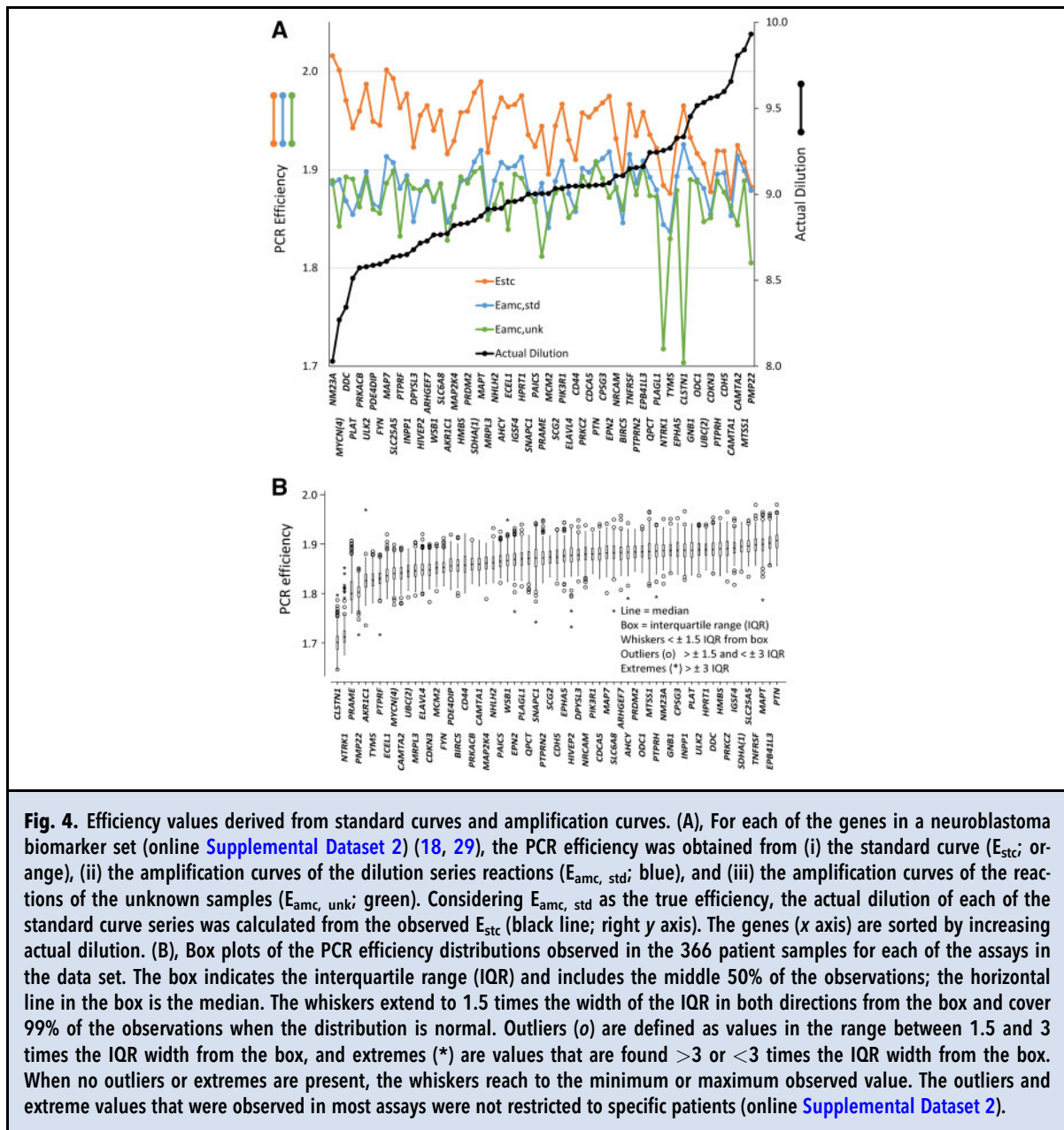


Fig. 3. Interpretation of gene expression ratios published as ΔC_q values. The graphs show “virtual” amplification curves with different C_q values (green symbols) and different PCR efficiencies (represented by the slope of the lines). The extrapolation of the exponential phase down to cycle 0, intersects the y axis at the target concentration. The example consists of 3 experimental conditions (I, II, and III) in which 2 targets are measured (genes A and B, in orange and blue, respectively). For each condition, the ΔC_q is -3 ($C_{q,A} - C_{q,B}$). (A–D), Amplification curves for different ranges of PCR efficiency values; solid lines when gene A has the highest efficiency, dotted lines when gene A has the lowest efficiency. The actual A/B gene expression ratio (inset tables) leading to a ΔC_q of -3 is calculated for 4 scenarios with different efficiency values. (A), Both genes amplify with an assumed PCR efficiency of 2. (B), One PCR efficiency differs 2% from 2. (C), PCR efficiencies between 1.93 and 2.05. (D), PCR efficiencies between 1.70 and 1.91. Note that for each gene, the ΔC_q between treatments I and II and between treatments II and III is -8 , which translates into an expression level difference of 256 times between conditions. See also online [Supplemental Excel File, Sheet 3](#).



interpret that result often implies completely wrong treatment effects. Reporting the result of calculations with Eq. 6, with the same assumption, also leads to invalid expression data. This large, and mostly ignored, influence of PCR efficiency on reported C_q values may account for the lack of reproducibility in published qPCR results. It should be noted that neither the calculation of relative expression between target and references nor the calculation of fold difference between treatment and control corrects for the bias introduced by assuming the same, or the maximal, efficiency for all

assays. Unbiased reporting of reliable, accurate, and reproducible qPCR results requires that the actual PCR efficiencies of the targets and the references be used in the analysis (4, 16, 17, 22, 23, 30).

How to Determine Amplification Efficiency?

The question that arises then is how to determine the PCR efficiency of the various targets to perform this efficiency-corrected analysis. The PCR efficiency of an assay is commonly derived from the slope of the standard

curve (8). To this end, C_q values are obtained from measurement of a dilution series with known dilution steps of the target (Fig. 1, B) and plotted against the $^{10}\log$ of the input concentration or dilution factor (Fig. 1, C). To understand why this graph can be used to derive the PCR efficiency, Eq. 2 has to be written in its logarithmic form and rearranged into the equation of a straight line fitted to the observed data:

$$C_q = \frac{\log(N_q)}{\log(E)} - \frac{1}{\log(E)} \log(\text{input}). \quad \text{Eq. 7 (8)}$$

From the slope of this line ($-1/\log(E)$), the efficiency can be derived as

$$E_{\text{stc}} = 10^{(-1/\text{slope})}. \quad \text{Eq. 8}$$

In this current review, the efficiency value derived from a standard curve is referred to as E_{stc} . This standard curve approach is valid only when the dilution steps are known and accurate, which in practice is not ensured (31). Random pipetting errors occur frequently, resulting in different standard curves and different efficiency values across PCR runs for the same assay (16, 31–34). Rasmussen (8) reported that replicate standard curves showed variation of up to 3% in their slope; with a PCR efficiency of 1.9, such 3% variation translates into E_{stc} values ranging from 1.86 to 1.94 (online Supplemental Background 4a; Supplemental Excel File, Sheet 7).

To avoid this variability in standard curves, alternative methods were developed to estimate the PCR efficiency of an assay. These methods use Eq. 1 to determine the efficiency from data points in the exponential phase of the individual amplification curves (9, 16, 32, 35–39). The logarithmic form of Eq. 1, $\log(N_c) = \log(N_0) + \log(E) \times c$, shows that in a log-linear plot of the amplification data, the slope constant of the straight line fitted to the exponential phase of a reaction is $\log(E)$ (16, 32, 37). Therefore, for each reaction, the PCR efficiency can be determined from this slope:

$$E_{\text{amc}} = 10^{\text{slope}} \quad \text{Eq. 9}$$

In this review, the efficiency value determined from the amplification curve of an individual reaction is referred to as E_{amc} . The best estimate of the PCR efficiency of an assay is obtained by calculating the arithmetic mean of the E_{amc} determined from all reactions of a specific target (16, 40, 41). Comparison of the standard curve approach with the methods to determine the PCR efficiency from amplification curves showed that PCR-Miner (35) and LinRegPCR (16) performed similarly with respect to sensitivity, reproducibility, and linearity. In that comparison, in which the E_{stc} results were considered to be correct, E_{amc} determined by

LinRegPCR showed biased results (18). However, as already discussed in that study, the claim that E_{stc} is unbiased stems from circular reasoning (Fig. 1, D). For any input series, the derived E_{stc} will result in an output that is perfectly correlated with the given input. However, when E_{stc} is wrong because of dilution errors (31), the results calculated for unknown samples will all be biased. Because E_{amc} follows directly from the PCR kinetics and is not affected by dilution of a standard, it is considered to be the actual efficiency. A prerequisite for determining an accurate E_{amc} is good-quality amplification data from which a valid fluorescence baseline can be estimated (16). Baseline estimation in qPCR systems is always based on the first, noisiest, fluorescence readings of the amplification reaction, resulting in variable and erroneous E_{amc} (online Supplemental Excel File, Sheet 1). LinRegPCR avoids the ground-phase cycles and determines a constant baseline for each reaction by reconstructing the longest straight exponential phase working downward from the plateau phase. When the plateau phase is present, this method can also handle data of probe-based assays, which often show high baselines and noisy ground phases (2, 42). Avoiding the noisy ground phase explains why, in the comparison of methods, LinRegPCR scored highest on reproducibility and sensitivity (18).

E_{stc} and E_{amc} Differ Because of Dilution Errors

The efficiency values derived from a standard curve (E_{stc} , Eq. 8) or determined from the amplification curves of the individual reactions of the dilution series (E_{amc} , Eq. 9) often differ. To illustrate this difference, we reanalyzed qPCR data of patients and dilution series for 63 assays (18) (online Supplemental Dataset 2). From this data set, we obtained (a) the efficiency derived from the standard curve (E_{stc}), (b) the mean efficiency determined from the amplification curves of the 15 reactions with standard dilutions ($E_{\text{amc, std}}$), and (c) the mean efficiency determined from the amplification curves of the 366 reactions of the unknown patient samples ($E_{\text{amc, unk}}$) (Fig. 4, A).

The difference between E_{stc} and $E_{\text{amc, std}}$ can be attributed to a systematic pipetting error (31). Such an error leads to an unintended actual dilution that differs from the intended dilution that was used to calculate the standard curve slope and thus leads to an incorrect E_{stc} . This dilution effect can be mathematically described as:

$$E_{\text{stc}} = E_{\text{amc, std}}^{\log(D)/\log(D(1+P))}. \quad \text{Eq. 10}$$

In this equation, $E_{\text{amc, std}}$ is the efficiency of the individual standard reactions, D the intended dilution, and P the fractional systematic pipetting error. The

derivation of this equation and the effects of different dilution errors on different PCR efficiencies are given in online [Supplemental Background 4b](#) ([Supplemental Excel File](#), Sheet 8). The use of the standard curve as a calibration curve for so-called absolute quantification ([Fig. 1, C](#)) also suffers from such dilution errors (online [Supplemental Background 5](#); [Supplemental Excel File](#), Sheets 9 and 10).

After rearrangement of Eq. 10 (online [Supplemental Background 4c](#)), the actual dilution used for preparation of the material in the standard curve reactions for each assay can be calculated ([Fig. 4, A](#)).

Although the standard curves in this data set were reported to be based on 10-fold dilution series (29), the actual dilutions were less, leading to higher E_{stc} .

To further illustrate how dilution errors affect E_{stc} , a 10% dilution error around an intended 10-fold dilution was simulated by preparing dilution series with 9-, 10- and 11-fold dilution steps (online [Supplemental Dataset 3](#)). For each dilution series, the observed C_q values were plotted against an assumed 10-fold dilution ([Fig. 5, A](#)), and from each standard curve, the E_{stc} was derived ([Fig. 5](#), inset table). The mean of the efficiencies determined from all 45 reactions showed that $E_{amc, std}$

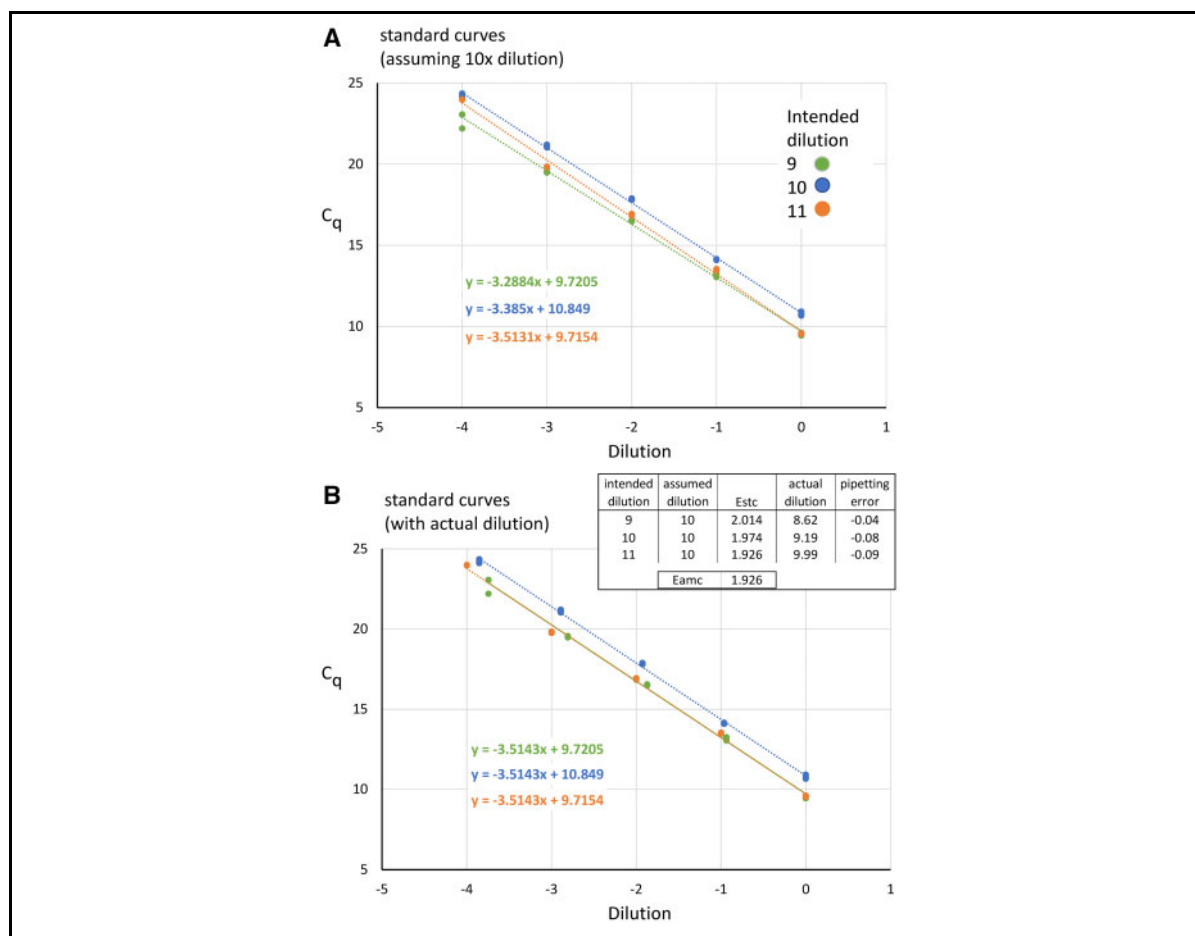


Fig. 5. Effect of the actual dilution on the standard curve-derived efficiency. To illustrate the effect of a systematic dilution error, three 5-step dilution series with intended dilutions of 9-, 10- and 11- fold dilution per step were prepared and measured in triplicate (online [Supplemental Dataset 3](#)). (A), For each dilution series, a standard curve was constructed with an assumed 10-fold dilution per step. The slopes are different and lead to different derived efficiency values (inset table). The table shows the PCR efficiencies (E_{stc}) derived from the standard curves in (A) for each of the dilution series. The table also gives the mean of the efficiency values (E_{amc}) determined from all 45 amplification curves. The E_{amc} did not differ significantly among the 3 dilution series (online [Supplemental Dataset 3](#)). The E_{stc} per dilution series and E_{amc} were used to calculate the actual dilution for each dilution series. (B), The standard curves for each dilution series constructed with the actual dilutions show the same slope for each series. The differences in the intercepts reflect the different amounts of material in the undiluted reactions of each series.

of this assay was 1.926 and was not different among dilution series (online [Supplemental Dataset 3](#)). With this $E_{\text{amc, std}}$ and the 3 E_{stc} values, the actual dilution per series was calculated to be within 4%–9% from the intended dilution. This result illustrates how difficult it is to reach the intended dilution for valid use of the standard curve approach, even for an experienced technician with calibrated pipets. When the actual dilution steps were used to construct the standard curves, the derived E_{stc} values were the same ([Fig. 5, B](#)).

E_{amc} Can Differ among Samples

The absence of context (i.e., nucleic acids and other biological compounds) in a PCR was shown to affect its efficiency (15). To illustrate how context affects qPCR analysis, the neuroblastoma biomarker dataset (online [Supplemental Dataset 2](#)) was reevaluated. The PCR efficiencies of these validated qPCR assays showed differences between the reactions of the standard curve and those of patient samples ($E_{\text{amc, std}}$ and $E_{\text{amc, unk}}$, respectively; [Fig. 4, A](#)). This difference is most likely due to the difference in context of the PCR: whereas the patient samples have a complex biological context, the standard curve samples consist of 55-bp oligonucleotides in bi-distilled water (43). Interestingly, the distribution of observed $E_{\text{amc, unk}}$ shows that for almost every assay, some patients show outlying or extreme efficiency values ([Fig. 4, B](#)). No systematic relations were found between the occurrence of outliers in assays or samples ([Supplemental Dataset 2](#)), indicating that the deviating PCR efficiencies occur randomly.

Similarly, the positive patient samples in the COVID-19 data set (online [Supplemental Dataset 1](#)) showed a wide range of PCR efficiencies ([Fig. 2, B and C](#)). Although this result is probably due to differences in context, such variability might also be due to the limited plateau/baseline ratio often encountered in probe-based assays (42). Indeed, the reactions with efficiency values below 1.6 displayed low-quality amplification curves with a low or no plateau (online [Supplemental Dataset 1](#)).

To further illustrate how difference in context affects PCR-based quantification, the data of 4 bovine pathogens in point-of-care diagnostics were reevaluated (online [Supplemental Dataset 4](#)). The qPCRs were performed on 4 different qPCR machines without technical replicates on nasal swabs collected in the field from 274 steers. E_{amc} was determined for all reactions showing amplification. For each target, E_{amc} shows overlapping distributions among machines ([Fig. 6, A](#); online [Supplemental Dataset 4](#)). The significant difference among machines shown for 2 targets was attributed to outliers. To determine whether such outliers were reproducible, for some randomly selected samples for the

qPCR were repeated 6 times. The PCR efficiency of 3 targets showed significant differences among samples with little variation among replicates per sample ([Fig. 6, B](#)). This high reproducibility of E_{amc} and the significant differences among samples illustrate that the observed E_{amc} is inherent to the samples. The fourth target showed high variability among and within samples (online [Supplemental Dataset 4](#)). One would expect that such different efficiencies would result from the presence of a PCR inhibitor or stimulator in some biological samples. However, comparison of the efficiencies per sample showed no significant correlation between targets, indicating that the variation in PCR efficiency is target and sample specific (online [Supplemental Dataset 4](#)).

Taken together, these results illustrate that in almost all assays, variability of PCR efficiency among biological samples is present. These differences may result from inherent variability among subjects and/or sampling procedures, which is unavoidable given time and cost constraints. In samples taken for clinical and point-of-care diagnostics, the presence of PCR inhibitors/stimulators cannot be ruled out (44). Moreover, PCR efficiency is affected by differences within the targeted sequence (45, 46), the sequences flanking the targeted sequence (47), or its conformation (48–50). Using the mean E_{amc} per assay, which was recommended for standardized laboratory experiments (18, 41), would lead to biased results for samples with deviating PCR efficiency. For such samples, reproducible and reliable quantification is best achieved using the E_{amc} per biological sample. However, doing so for the low-quality reactions in the COVID-19 data set, most of which combine a low PCR efficiency with a high C_q value ([Fig. 2, B](#)), resulted in an impossibly high number of targets per reaction ([Fig. 2, D](#)). The large proportion of such samples in this data set shows that, even when individual PCR efficiencies are used in the calculation, this assay cannot be used for quantitative purposes.

Absolute Quantification without Dilution of the Standard

The issues discussed so far show that the PCR efficiency is affected by (a) systematic dilution errors in preparing a standard curve, (b) random pipetting errors in the standard curve samples, (c) the sequence and context of the target, and (d) unknown components inherent to the biological sample. Therefore, unbiased efficiency-corrected absolute quantification would benefit from a protocol in which dilution of the standard is avoided and the actual PCR efficiencies of the standard and unknown reactions are used in the calculations. The 1-point calibration method fulfils these requirements (51). This method uses a single, independently defined

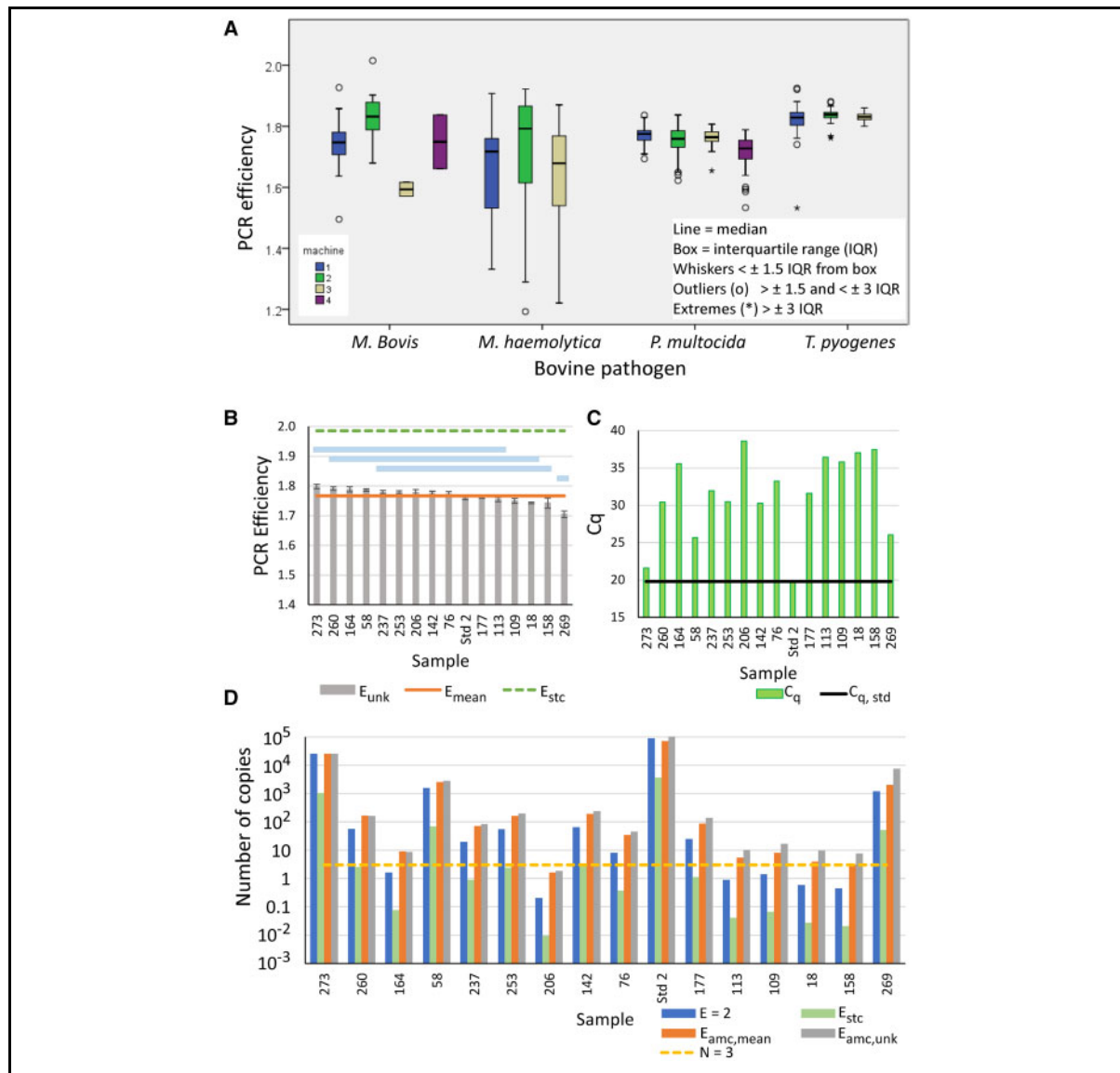


Fig. 6. On-site measurement of bovine pathogens. *Mycoplasma bovis*, *Trueperella pyogenes*, *Mannheimia haemolytica*, and *Pasturella multocida* were measured in nasal swaps of 274 steers using 4 different qPCR machines of the same brand (online Supplemental Dataset 4). (A), Box plots of the observed PCR efficiency per pathogen and per machine. For each target, the distributions are overlapping (Supplemental Dataset 4). Statistical comparison showed that the difference among machines was significant for *M. bovis* and *P. multocida* (1-way ANOVA; both $P < 0.001$) but not for *M. haemolytica* and *T. pyogenes* (1-way ANOVA; $P = 0.430$ and $P = 0.192$, respectively). However, these differences were due to outlying individual samples (see legend Fig. 4, B). In (B), (C), and (D), results for *P. multocida* are shown for 15 randomly selected steers and a standard (x axis). See Supplemental Dataset 4 for the other targets. (B), Bar graphs of the observed PCR efficiencies (mean \pm SEM) of the *P. multocida* target in 6 technical replicate measurements of the standard (std) and selected biological samples (numbers). The horizontal green dotted line indicates the efficiency derived from the standard curve (E_{stc}), and orange line shows the mean of the efficiencies determined from the amplification curves of all samples (E_{mean}). The blue horizontal bars indicate homogeneous subsets of samples that do not differ significantly from each other; nonoverlapping parts of the blue bars indicate sample(s) that differ significantly at $P = 0.05$ (ANOVA with multiple comparison of groups: Student-Newman-Keuls test). (C), Bar graphs of C_q values observed in the standard and unknown samples for the *P. multocida* target. The horizontal black line indicates the C_q value of the standard. (D), Number of copies for the *P. multocida* target in each of the unknown samples calculated using 4 different PCR efficiency values and the observed C_q value per sample (see text for details). The *P. multocida* standard contained 10^5 copies of the target. The horizontal orange dotted line indicates the limit of detection of qPCR.

standard with a known number of copies of the target amplified in the same PCR run as the unknown samples. The PCR $E_{\text{amc, std}}$ and $E_{\text{amc, unk}}$ are determined from their respective amplification curves. After setting a common threshold (N_q), the C_q values are determined. Because the threshold is the same for both reactions, $N_q = N_{0, \text{unk}} E_{\text{amc, unk}}^{C_{q, \text{unk}}}$ and $N_q = N_{0, \text{std}} E_{\text{amc, std}}^{C_{q, \text{std}}}$ (Eq. 2), and thus $N_{0, \text{std}} E_{\text{amc, std}}^{C_{q, \text{std}}} = N_{0, \text{unk}} E_{\text{amc, unk}}^{C_{q, \text{unk}}}$. Rearrangement of the latter equality (online Supplemental Background 6a) shows that the target quantity of the unknown sample can be calculated with:

$$N_{0, \text{unk}} = N_{0, \text{std}} \frac{E_{\text{amc, std}}^{C_{q, \text{std}}}}{E_{\text{amc, unk}}^{C_{q, \text{unk}}}}. \quad [\text{Eq. 11}] \quad (51)$$

$E_{\text{amc, unk}}$ in Eq. 11 can be the mean efficiency for all unknown samples or the mean efficiency of technical replicates per sample when $E_{\text{amc, unk}}$ differs significantly among samples. Moreover, it is important that $E_{\text{amc, std}}$ and $C_{q, \text{std}}$ are based on a sufficient number of replicate reactions to ensure that the actual number of copies in the standard reactions is the same as the predefined $N_{0, \text{std}}$. Considering the Poisson sampling variation and allowing for a 6% pipetting error, 95% precision of a 1000-copy standard (with a C_q value of approximately 28 cycles) can be reached with 6 replicate reactions (online Supplemental Background 6b; Supplemental Excel File, Sheet 11). Technical replicates of unknown samples may be outside the scope of the diagnostic test because of time and cost limitations. In that case, the C_q and the efficiency per sample might still enable more accurate reporting of the individual unknown target concentration than an efficiency per assay that is assumed to be correct.

Comparison of Calculation Methods

To illustrate and compare the different ways to calculate the gene expression ratio between unknown samples and a standard, one of the bovine pathogens from the replicate measurements of different steers was used (online Supplemental Dataset 4). For each biological sample and standard, the values for PCR efficiency (Fig. 6, B) and C_q (Fig. 6, C) of the target are shown. The ΔC_q between samples and standard is the difference between the bars and the horizontal line ($C_{q, \text{std}}$). The number of copies of the target in the samples was calculated using this ΔC_q and (a) assumption of maximal PCR efficiency ($E = 2$), (b) the PCR E_{stc} , and (c) the PCR E_{mean} . Last, the number of copies was calculated using Eq. 11 with the C_q and E_{amc} of the samples as well as the standard (Fig. 6, D; online Supplemental Dataset 4). Comparison of the different colored bars with the gray bars shows large and different biases among subjects. These biases

are introduced by assuming the maximal efficiency or the same efficiency for every sample and differ per sample because the bias depends on the actual C_q and PCR efficiency of the sample. The limit of detection of qPCR, defined as the number of target molecules that have to be present on average in a reaction to show amplification in 95% of the technical replicates, is 3 copies (3, 4, 52). In particular, the assumption that the efficiency is maximal leads to target numbers that are far below this limit of detection. This comparison shows that in the calculation of the reported qPCR result, the actual efficiency of the standard and the unknown samples should be used to avoid bias introduced by an efficiency that is assumed, or assumed to be correct.

Recommendations for Extensions to the MIQE Guidelines

The MIQE guidelines provide a checklist of essential and desirable information that should be reported to enable the reviewer to judge the validity of the study and the reader to repeat the experiment and reproduce the results (4).

With respect to reporting C_q -based results, MIQE already states that “the most popular method is not necessarily the most appropriate” and refers to Eq. 5 as an alternative quantitative model (23). The guidelines state that the PCR efficiencies required for this alternative approach “must be established by means of a calibration curve.” However, when PCR efficiencies differ between assays, the “calculations of relative concentrations will be inaccurate.” Despite this reticence, it is common practice to report qPCR results as (a) only C_q values, (b) C_q values and E_{stc} but calculations with $E = 2$ (Eq. 6), (c) fold difference calculated with C_q values and E_{stc} (Eq. 5), or (d) target quantity calculated with C_q and E_{stc} or E_{amc} (Eq. 3). Only the last 2 results are efficiency corrected but may still be biased because of dilution errors in the standard curve.

Based on the data presented in this review, we propose to add the option to determine the E_{amc} to the MIQE checklist. The variation in the reported E_{amc} serves as a quality criterion; the SD indicates its reproducibility, and the SEM indicates its precision. These variation measures are provided by the methods used to determine E_{amc} (16, 35). When technical replicates per biological sample are measured, 1-way ANOVA can be used to compare the mean E_{amc} per sample to identify samples with deviating efficiency.

Moreover, to ensure valid and reproducible qPCR reports, the description of how the PCR efficiency is used to calculate efficiency-corrected qPCR results should be an essential item in the MIQE checklist. Adding this requirement to MIQE sidesteps assumptions

on equality of PCR efficiency among assays, samples, and reactions and avoids the variability that the “ $\Delta\Delta C_q$ simplification” introduced into the qPCR field. When the starting concentration (N_0 ; Eq. 3) of the target (shown as *tar*; *ref* is reference) is determined, the gene expression ratio ($N_{0, \text{tar}}/N_{0, \text{ref}}$) per condition and the fold change among experimental conditions ($(N_{0, \text{tar}}/N_{0, \text{ref}})_{\text{treated}}/(N_{0, \text{tar}}/N_{0, \text{ref}})_{\text{control}}$) are easy calculations. The final result is similar to that of the classic efficiency-corrected gene expression equation (23) and even the same when E_{amc} of target and reference are used in Eq. 5. However, the major advantage of first calculating N_0 per reaction is that intermediate results become visible and deviating reactions, samples, or assays can easily be pinpointed.

For absolute calibration, MIQE requires reporting of details of the calibration curve. However, for clinical and diagnostic application of qPCR, it would be desirable to extent of the MIQE checklist with the details of single standard calibration (Eq. 11)—that is, $N_{0, \text{std}}$, $E_{\text{amc, std}}$, $C_{q, \text{std}}$, and number of replicate reactions of the standard.

Conclusion

This review shows comprehensively that reporting qPCR results as C_q , ΔC_q or $\Delta\Delta C_q$ with the assumption that the PCR efficiency is 100% is circumspect at best and meaningless at worst. Therefore, we recommend that only efficiency-corrected results from qPCR experiments be published and that the MIQE guidelines be extended accordingly. Moreover, because biological samples used in diagnostics are collected under challenging and often non-standardized conditions, we recommend that the reported efficiency-corrected results are calculated with an efficiency determined per sample. When the PCR efficiency per sample can be reliably determined, the combination with single standard calibration results in an unbiased efficiency-corrected absolute copy number that can be reported reliably for meaningful diagnostics or biological interpretation.

Supplemental Material

Supplemental material is available at *Clinical Chemistry* online.

Nonstandard Abbreviations: qPCR, quantitative real-time PCR; C_q , quantification cycle; MIQE, Minimum Information for Publication of Quantitative Real-Time PCR Experiments; N_c , number of target copies after c cycles; N_0 , starting number of targets; E , efficiency; N_q , quantification threshold; E_{std} , efficiency derived from a standard curve; E_{amc} , efficiency determined from the amplification curve; $E_{\text{amc, std}}$, efficiency determined from the amplification curves of reactions with standard dilutions; $E_{\text{amc, unk}}$, efficiency determined from the amplification curves of reactions unknown patient samples; E_{mean} , mean of efficiencies determined from the amplification curves per assay.

Author Contributions: All authors confirmed they have contributed to the intellectual content of this paper and have met the following 4 requirements: (a) significant contributions to the conception and design, acquisition of data, or analysis and interpretation of data; (b) drafting or revising the article for intellectual content; (c) final approval of the published article; and (d) agreement to be accountable for all aspects of the article thus ensuring that questions related to the accuracy or integrity of any part of the article are appropriately investigated and resolved.

J.M. Ruijter, statistical analysis; J.C. Quinn, financial support, provision of study material or patients; R. van Houdt, provision of study material or patients; M.J.B. van den Hoff, financial support, administrative support, provision of study material or patients.

Authors' Disclosures or Potential Conflicts of Interest: Upon manuscript submission, all authors completed the author disclosure form. Disclosures and/or potential conflicts of interest:

Employment or Leadership: A.N. Szentirmay, Gene Target Solutions.

Consultant or Advisory Role: A.N. Szentirmay, Gene Target Solutions.

Stock Ownership: None declared.

Honoraria: None declared.

Research Funding: R.J. Barnewall was supported by PhD scholarship awards from Charles Sturt University and Meat and Livestock Australia. J.C. Quinn, I.B. Marsh, and R.J. Barnewall were supported by funding from Meat and Livestock Australia Donor Company project P.PSH.0805.

Expert Testimony: A.N. Szentirmay, Gene Target Solutions.

Patents: None declared.

Other Remuneration: R.J. Barnewall, Meat and Livestock Australia, Australian Government Research Training Program—Full time scholarship.

Acknowledgments: J.M. Ruijter and M.J.B. van den Hoff wish to thank Axel van den Hoff for checking the derivation of equations presented in the online [Supplemental Background](#). We thank Jo Vandesompele (Ghent University) for permission to use the data set with amplification data of 63 genes.

References

- Wittwer CT, Herrmann MG, Moss AA, Rasmussen RP. Continuous fluorescence monitoring of rapid cycle DNA amplification. *BioTechniques* 1997;22:130-8.
- Ruijter JM, Lorenz P, Tuomi JM, Hecker M, van den Hoff MJ. Fluorescent-increase kinetics of different fluorescent reporters used for qPCR depend on monitoring chemistry, targeted sequence, type of DNA input and PCR efficiency. *Mikrochim Acta* 2014;181: 1689-96.
- Kralik P, Ricchi M. A basic guide to real time PCR in microbial diagnostics: definitions, parameters, and everything. *Front Microbiol* 2017;8:108.
- Bustin SA, Benes V, Garson JA, Hellemans J, Huggett J, Kubista M, et al. The MIQE guidelines: minimum information for publication of quantitative real-time PCR experiments. *Clin Chem* 2009;55:611-22.
- Taylor SC, Nadeau K, Abbasi M, Lachance C, Nguyen M, Fenrich J. The ultimate qPCR experiment: producing publication quality, reproducible data the first time. *Trends Biotechnol* 2019;37:761-74.
- Nolan T, Hands RE, Bustin SA. Quantification of mRNA using real-time RT-PCR. *Nat Protoc* 2006;1:1559-82.
- Abdel Nour AM, Pfaffl MW, editors. MIQE and qPCR: how to apply the MIQE guidelines—a visual interactive and practical guide. 4th Ed. Freising (Germany): bioMCC; 2020. https://www.gene-quantification.de/MIQE_qPCR_iBook_v4_June_2020.pdf

8. Rasmussen. Quantification on the LightCycler instrument. In: S Meuer, C Wittwer, K Nakagawara, editors. *Rapid cycle Real-Time PCR: methods and applications*. Heidelberg (Germany): Springer; 2001. p. 21–34.
9. Rutledge RG, Stewart D. Critical evaluation of methods used to determine amplification efficiency refutes the exponential character of real-time PCR. *BMC Mol Biol* 2008;9:96.
10. Scheffe JH, Lehmann KE, Buschmann IR, Unger T, Funke-Kaiser H. Quantitative real-time RT-PCR data analysis: current concepts and the novel "gene expression's CT difference" formula. *J Mol Med (Berl)* 2006;84:901–10.
11. Huggett JF, Benes V, Bustin SA, Garson JA, Harris K, Kammel M, et al. Cautionary note on contamination of reagents used for molecular detection of SARS-CoV-2. *Clin Chem* 2020;66:1369–72.
12. Ritz C, Spiess AN. qPCR: an R package for sigmoidal model selection in quantitative real-time polymerase chain reaction analysis. *Bioinformatics* 2008;24:1549–51.
13. Shipley G. Assay design for real-time qPCR. In: T Nolan, SA Bustin, editors. *PCR technology: current innovations*. 3rd Ed. London (UK): CRC Press; 2013. p. 177–99.
14. de Ronde MW, Ruijter JM, Lanfear D, Bayes-Genis A, Kok M, Creemers E, et al. Practical data handling pipeline improves performance of qPCR-based circulating miRNA measurements. *RNA* 2017;23:811–21.
15. Ruiz-Villalba A, van Pelt-Verkuil E, Gunst QD, Ruijter JM, van den Hoff MJ. Amplification of nonspecific products in quantitative polymerase chain reactions (qPCR). *Biomol Detect Quantif* 2017;14:7–18.
16. Ruijter JM, Ramakers C, Hoogaars WM, Karlen Y, Bakker O, van den Hoff MJ, Moorman AF. Amplification efficiency: linking baseline and bias in the analysis of quantitative PCR data. *Nucleic Acids Res* 2009;37:e45.
17. Hellemans J, Mortier G, De PA, Speleman F, Vandesompele J. qBase relative quantification framework and software for management and automated analysis of real-time quantitative PCR data. *Genome Biol* 2007;8:R19.
18. Ruijter JM, Pfaffl MW, Zhao S, Spiess AN, Boggy G, Blom J, et al. Evaluation of qPCR curve analysis methods for reliable biomarker discovery: bias, resolution, precision, and implications. *Methods* 2013;59:32–46.
19. Thellin O, Zorzi W, Lakaye B, De Borman B, Coumans B, Hennen G, et al. Housekeeping genes as internal standards: use and limits. *J Biotechnol* 1999;75:291–5.
20. Thellin O, ElMoualij B, Heinen E, Zorzi W. A decade of improvements in quantification of gene expression and internal standard selection. *Biotechnol Adv* 2009;27:323–33.
21. Vandesompele J, De Preter K, Pattyn F, Poppe B, Van Roy N, De Paepe A, Speleman F. Accurate normalization of real-time quantitative RT-PCR data by geometric averaging of multiple internal control genes. *Genome Biol* 2002;3:RESEARCH0034.
22. Ruiz-Villalba A, Mattiotti A, Gunst QD, Cano-Ballesteros S, van den Hoff MJ, Ruijter JM. Reference genes for gene expression studies in the mouse heart. *Sci Rep* 2017;7:24.
23. Pfaffl MW. A new mathematical model for relative quantification in real-time RT-PCR. *Nucleic Acids Res* 2001;29:e45.
24. Nordgard O, Kvaloy JT, Farnen RK, Heikkila R. Error propagation in relative real-time reverse transcription polymerase chain reaction quantification models: the balance between accuracy and precision. *Anal Biochem* 2006;356:182–93.
25. Pfaffl MW. REST 2009 software user guide. Corbett Research, Hilden (Germany): Qiagen; 2009. https://www.gene-quantification.de/REST_2009_Software_User_Guide.pdf (Accessed January 2020).
26. Page RB, Stromberg AJ. Linear methods for analysis and quality control of relative expression ratios from quantitative real-time polymerase chain reaction experiments. *ScientificWorldJournal* 2011;11:1383–93.
27. Livak KJ, Schmittgen TD. Analysis of relative gene expression data using real-time quantitative PCR and the $2^{-\Delta\Delta CT}$ method. *Methods* 2001;25:402–8.
28. Yuan JS, Wang D, Stewart CN. Jr., Statistical methods for efficiency adjusted real-time PCR quantification. *Biotechnol J* 2008;3:112–23.
29. Vermeulen J, de Preter K, Naranjo A, Vercruyse L, Van Roy N, Hellemans J, et al. Predicting outcomes for children with neuroblastoma using a multigene-expression signature: a retrospective SIOOPEN/COG/GPOH study. *Lancet Oncol* 2009;10:663–71.
30. Meijerink J, Mandigers C, van de Locht L, Tonissen E, Goodsaid F, Raemaekers J. A novel method to compensate for different amplification efficiencies between patient DNA samples in quantitative real-time PCR [English. *J Mol Diagn* 2001;3:55–61.].
31. Ruijter JM, van den Hoff MJ. The importance of efficiency-correlation in qPCR. In: AM Abdel Nour, MW Pfaffl, editors. *MIQE and qPCR iBook: how to apply the MIQE guidelines—a visual, interactive and practical qPCR guide*. 3rd Ed. Freising (Germany): bioMCC; 2019: 246–265.
32. Ramakers C, Ruijter JM, Lekanne Deprez RH, Moorman AFM. Assumption-free analysis of quantitative real-time polymerase chain reaction (PCR) data. *Neurosci Lett* 2003;339:62–6.
33. Towe S, Kleideidam K, Schloter M. Differences in amplification efficiency of standard curves in quantitative real-time PCR assays and consequences for gene quantification in environmental samples. *J Microbiol Methods* 2010;82:338–41.
34. Smith CJ, Osborn AM. Advantages and limitations of quantitative PCR (Q-PCR)-based approaches in microbial ecology. *FEMS Microbiol Ecol* 2009;67:6–20.
35. Zhao S, Fernald RD. Comprehensive algorithm for quantitative real-time polymerase chain reaction. *J Comput Biol* 2005;12:1047–64.
36. Tichopad A, Dilger M, Schwarz G, Pfaffl MW. Standardized determination of real-time PCR efficiency from a single reaction set-up. *Nucleic Acids Res* 2003;31:e122.
37. Peirson SN, Butler JN, Foster RG. Experimental validation of novel and conventional approaches to quantitative real-time PCR data analysis. *Nucleic Acids Res* 2003;31:e73.
38. Lievens A, Van Aelst S, Van den Bulcke M, Goetghebeur E. Enhanced analysis of real-time PCR data by using a variable efficiency model: FPK-PCR. *Nucleic Acids Res* 2012;40:e10.
39. Spiess AN, Feig C, Ritz C. Highly accurate sigmoidal fitting of real-time PCR data by introducing a parameter for asymmetry. *BMC Bioinformatics* 2008;9:221.
40. Karlen Y, McNair A, Perseguers S, Mazza C, Mermod N. Statistical significance of quantitative PCR. *BMC Bioinformatics* 2007;8:131.
41. Cikos S, Bukovska A, Koppel J. Relative quantification of mRNA: comparison of methods currently used for real-time PCR data analysis. *BMC Mol Biol* 2007;8:113.
42. Tuomi JM, Voorbraak F, Jones DL, Ruijter JM. Bias in the C_q value observed with hydrolysis probe based quantitative PCR can be corrected with the estimated PCR efficiency value. *Methods* 2010;50:313–22.
43. Vermeulen J, Pattyn F, De Preter K, Vercruyse L, Derveaux S, Mestdagh P, et al. External oligonucleotide standards enable cross laboratory comparison and exchange of real-time quantitative PCR data. *Nucleic Acids Res* 2009;37:e138.
44. Kontanis EJ, Reed FA. Evaluation of real-time PCR amplification efficiencies to detect PCR inhibitors. *J Forensic Sci* 2006;51:795–804.
45. Polz MF, Cavanaugh CM. Bias in template-to-product ratios in multitemplate PCR. *Appl Environ Microbiol* 1998;64:3724–30.
46. Lefever S, Pattyn F, Hellemans J, Vandesompele J. Single-nucleotide polymorphisms and other mismatches reduce performance of quantitative PCR assays. *Clin Chem* 2013;59:1470–80.
47. Hansen MC, Tolker-Nielsen T, Givskov M, Molin S. Biased 16S rDNA PCR amplification caused by interference from DNA flanking the template region. *Fems Microbiol Ecol* 1998;26:141–9.
48. Lin CH, Chen YC, Pan TM. Quantification bias caused by plasmid DNA conformation in quantitative real-time PCR assay. *PLoS One* 2011;6:e29101.
49. Bru D, Martin-Laurent F, Philippot L. Quantification of the detrimental effect of a single primer-template mismatch by real-time PCR using the 16S rRNA gene as an example. *Appl Environ Microbiol* 2008;74:1660–3.
50. Ishii K, Fukui M. Optimization of annealing temperature to reduce bias caused by a primer mismatch in multitemplate PCR. *Appl Environ Microbiol* 2001;67:3753–5.
51. Brankatschk R, Bodenhausen N, Zeyer J, Burgmann H. Simple absolute quantification method correcting for quantitative PCR efficiency variations for microbial community samples. *Appl Environ Microbiol* 2012;78:4481–9.
52. Forootan A, Sjoback R, Bjorkman J, Sjogreen B, Linz L, Kubista M. Methods to determine limit of detection and limit of quantification in quantitative real-time PCR (qPCR). *Biomol Detect Quantif* 2017;12:1–6.